Predicting UHPC Structural Response at Ultimate Limit State through Numerical Simulation Technique

Mandeep Pokhrel

Ph.D. Candidate, New Jersey Institute of Technology, Newark, NJ

Matthew J. Bandelt

Assistant Professor, New Jersey Institute of Technology, Newark, NJ

Keywords:

Abstract: Ultra-high performance concrete (UHPC) is being considered as an alternative ductile material to be used in the expected plastic hinge regions of structural components in buildings and bridges. Although several experimental studies of reinforced UHPC structural elements have been conducted for proof-of-concept seismic application, quantification of the plastic hinge length and associated rotation at ultimate limit states remains the most significant aspect for the ductile design of UHPC components in new structures. To that end, this study utilizes two-dimensional finite element models incorporating recently developed bond-slip constitutive model, which aids in simulating multiple damage states, such as yielding of reinforcement and reinforcement fracture. Several finite element models with variations in geometrical properties and loading scheme were simulated to compute the equivalent plastic hinge length values for reinforced UHPC flexural members. The existing empirical equations available for reinforced concrete and reinforced high-performance fiber-reinforced cementitious composite (HPFRCC) were found to over-predict the equivalent plastic hinge length in reinforced UHPC members. In addition, a mechanics-based approach was used to estimate the ultimate rotation capacity utilizing the plastic hinge length values obtained from numerical simulation techniques. This study can be used as starting point to develop a more robust empirical expression of plastic hinge length for reinforced UHPC flexural members and formulate a simplified approach to compute non-linear modeling parameters for displacement-based seismic design of UHPC structural components.

Keywords: reinforced UHPC, finite element analysis, plastic hinge length, sectional analysis, plastic rotation, ultimate rotation

1. Introduction and Background

With the improved understanding of seismic behavior of structures, design principles based on displacement approaches are being widely adopted in lieu of traditional force-based approach. Displacement-based design approach requires inelastic modeling of structural components to measure the performance metrics in terms of displacement/rotation, which cannot be accomplished through elastic modeling as in the case in force-based approach (Priestley et al.). Therefore, it is imperative to correctly quantify the equivalent plastic hinge length to calculate the displacement/rotation capacity so that it can be used in the inelastic modeling of structures subjected to extreme loadings such as seismic loading. Another important aspect in displacement-based design is the ability of a structural component to undergo large inelastic displacement without losing the load carrying capacity. This ability to undergo large deformations depends on the performance of the plastic hinge region where the entire inelastic damage concentrates. The use of traditional concrete in potential plastic hinge regions of structural components has demonstrated lower deformation capacity and energy absorption capacity due to early spalling of cover, longitudinal reinforcement buckling and concrete core crushing. To reduce such damage, alternative cementitious material such as high performance fiber-reinforced cementitious composite (HPFRCC) have been engineered by the researchers to construct more ductile, durable and resilient structures under extreme loading. HPFRCCs can be distinguished from other cement-based ductile materials based on their unique pseudo tensile strain-hardening behavior with multiple distributed cracking under uniaxial tension test (Reinhardt). HPFRCCs have several classes of cementitious materials tailored according to the specific loading requirement, and among them ultra-high performance concrete (UHPC) is a special class of cementitious material which is characterized by extremely high tensile strength ($5 < f_t < 11\ MPa$), compressive strength ($112 < f_t < 210\ MPa$), and energy absorption capacity (Graybeal).

Table 1. Empirical expressions of plastic hinge length

Reference	Expressions	Element	Loading
Mattock	$0.5d + 0.05z$	R/C Beam	Monotonic
Paulay and Priestley	$0.08d + 0.022f_y d_b$	R/C Beam & Column	Monotonic
Naaman et al.	$0.5(1.06d + 0.13\rho V)d$	R/HPFRCC Beam	Monotonic
Tariq, Jampole, and Bandelt	$(0.3 + 0.18\rho)d$	R/HPFRCC Beam	Cyclic

Although UHPC has several attractive properties to be adopted as a construction material, the high cost associated with its production has restricted its widespread use in the construction industry. However, UHPC can be prudently used in critical regions such as plastic hinge regions of beams/columns to significantly improve ductility and strength, while minimizing future repair cost. Experimental studies using steel reinforced UHPC have been conducted to understand the bond behavior between steel and UHPC matrix, performance under various mechanical stresses such as flexure, shear, torsion, and resistance under extreme loading such as impact and blast (Yoo and Yoon). Recent experimental studies shows that the failure mode in steel (mild or high strength) reinforced UHPC is primarily due to the fracture of longitudinal reinforcement rather than crushing of compression zone (Yoo and Yoon; Hung and Chueh). This is attributed to the high resistance of cementitious matrix towards the formation of splitting crack leading to crack localization, which has been observed in other classes of HPFRCC as well (Matthew J Bandelt and Billington). In another study conducted by Pokhrel and Bandelt, it was found that there is exponential increment of plastic strain in the tensile reinforcement at the dominant localized crack, which indicates that the spread of plasticity and the mechanics behind the formation of the plastic hinge region in reinforced UHPC will be different compared to that of the conventional reinforced concrete flexural members.

While there have been research studies exploring the applicability and structural behavior of UHPC, there is still limited investigation related to quantifying the plastic hinge length and associated plastic rotation in UHPC structural elements such as beam or column. The plastic hinge region of reinforced UHPC is an inelastic region with highly non-linear interaction between reinforcement and UHPC matrix, and characterized by crack localization. The formation and nature of plastic hinge region in a UHPC member will govern its ultimate load carrying capacity, ultimate displacement/rotation and energy absorption capacity under extreme loadings. The plastic hinge length, sometimes referred to as “equivalent plastic hinge length”(L_p) is the fictitious length over which plastic curvature is assumed to be constant, such that the integrated area under the actual plastic curvature is equal to the area under assumed curvature (Paulay and Priestley). The concept of plastic hinge length provides a simplified mathematical approach to calculate plastic rotation capacity (θ_p) of a member undergoing large inelastic deformation using cross-sectional curvature analysis. If the elastic or yield rotation capacity (θ_y) is calculated using elastic deflection theory, then the ultimate rotation capacity (θ_u) can be easily computed using Equation 1.

$$\theta_u = \theta_y + \theta_p = \frac{1}{2}\phi_y L_s + (\phi_u - \phi_y) L_p \tag{1}$$

Where L_s is the shear-span length, ϕ_y and ϕ_u are the sectional curvatures of the structural member at service (i.e., yielding of reinforcement) and ultimate ((i.e., fracture of reinforcement) level respectively. Table 1 summarizes several empirical equations of equivalent plastic hinge length developed for reinforced concrete and reinforced HPFRCC structural elements under different loading. The expressions are based on regression analysis of either experimental, numerical or hybrid studies with variation in mechanical and structural properties. It can be observed from the equations that the control variables are associated with two distinct phenomena, namely: (a) moment gradient related with the shear-span or flexural depth, and (b) tensile strain penetration through bond-slip mechanism inside the joint or foundation.

This study intends to investigate the plastic hinge region and ultimate rotation capacity in reinforced UHPC members through numerical simulation and sectional analysis. Numerical simulation results were used to compute curvature distribution along the shear-span of the reinforced UHPC members. Using numerical integration and sectional analysis, equivalent plastic hinge lengths were calculated for reinforced UHPC flexural members and compared with the values obtained from existing empirical models. Using mechanics-based approach, ultimate rotation capacity was calculated utilizing the equivalent plastic hinge length values and compared with ultimate rotation obtained from numerical simulation.

2. Numerical Simulation

2.1. Finite Element Models

Two dimensional finite element models with two different boundary conditions were simulated using DIANA FEA Version 10.2 (DIANAFEA) as shown in Figure 1. The setup and geometrical properties were selected as they are representative of reinforced HPFRCC experiments tested to large displacements under monotonic and cyclic loading including the fracture of reinforcement. Elastic support and loading plates were used at both sides of the beams to prevent inelastic stress concentration at the interface between plates and UHPC beam elements. Vertical and lateral springs were modeled as uniaxial springs at the base of the support plates. Foundation beams with dimension ($l\ x\ b\ x\ h$) of 800 mm x 130 mm x 380 mm were used as the base support for the cantilever beams.

To capture the variability in length of plastic hinge region in reinforced UHPC members with change of moment gradient along the shear span, two different shear spans (L_s) equal to 650 mm and 1080 mm length were chosen corresponding shear span-to-depth ratio (L_s/d) of 4.06 and 6.75 respectively. Symmetrical longitudinal reinforcement on top and bottom sides with areas 142 mm^2, 258 mm^2 and 398 mm^2 corresponding to reinforcement ratios (ρ) of 0.70%, 1.25% and 1.90% were used in different specimens to account for the variation due to the longitudinal reinforcement. Two types of loading scenario (i.e. monotonic load and reversed cyclic load) were used to formulate plastic hinge length. Monotonic load was applied using incremental displacement-based approach at a step size of 0.25 mm and reversed cyclic load was applied using FEMA 461 loading protocol until the fracture of longitudinal reinforcement or crushing of UHPC was observed. Therefore, a total of 24 finite element models were simulated in this study with variability in loading scheme, boundary condition, shear span and reinforcement ratio $(2\ x\ 2\ x\ 2\ x\ 3 = 24)$.

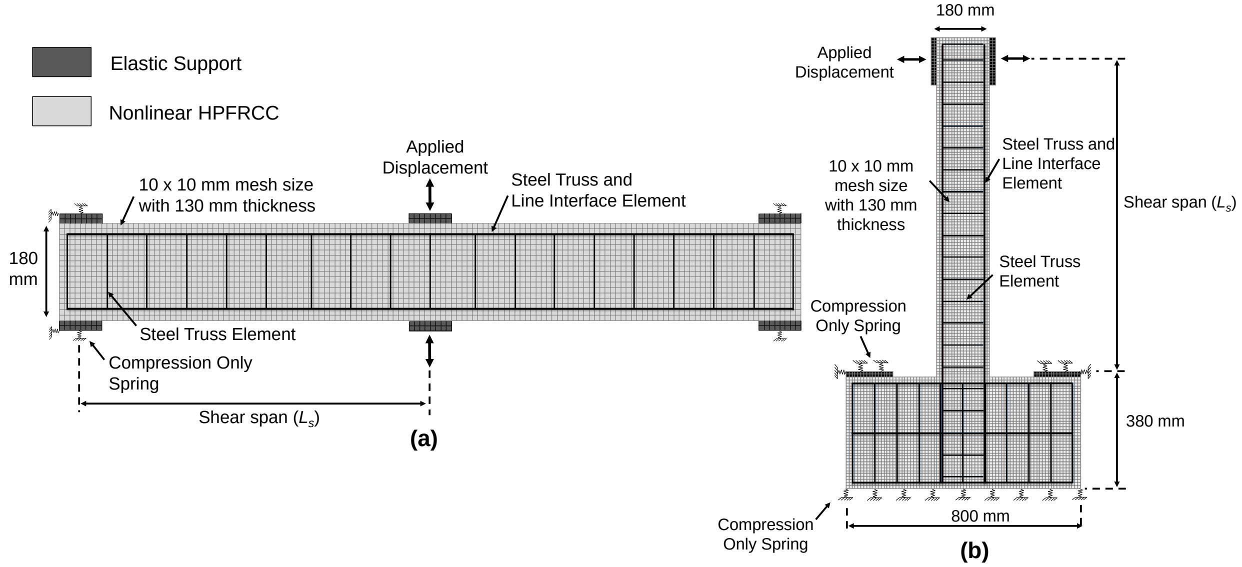

Figure 1. Finite Element Models (a) simply supported beam (b) cantilever beam

2.1. Material models, properties and analysis parameters

The mechanical properties for UHPC were chosen based on tension and compression tests available in the literature (Wille and Naaman; Russell and Graybeal). A total strain-based fixed-crack model was used as the constitutive model to simulate the behavior of UHPC materials (Feenstra et al.). A constant shear retention factor of 1% was used to simulate the transfer of shear stress across the cracks. The UHPC materials were modeled using an eight-noded quadratic plane stress element. The size of each element was $10\ x\ 10$ mm and the thickness was 130 mm. A $3\ x\ 3$ Gauss integration scheme and quadratic interpolation was used in the finite element numerical formulation. The material tensile response was modeled using an idealized multi-linear stress-strain curve as shown in Figure 2(a). The tensile model parameters were obtained from uniaxial tensile test data conducted by Wille and Naaman, and are summarized in Table 2. The ultimate tensile strain (ε_{tu}) was based on the experimentally observed tensile fracture energy and was calculated using a linear softening model as shown in Equation 2.

$$\varepsilon_{tu} = 2\frac{G_f}{h}\frac{1}{f_t} + \varepsilon_{tp} \qquad (2)$$

In Equation 2, h is the crack bandwidth which is equal to $\sqrt{A}$, where A is the area of an individual plane stress element. As only one mesh discretization is presented in this paper, crack-band approach was used to eliminate the problem related with mesh dependency. The compression response of the UHPC materials was modeled using a parabolic stress-strain curve based on compressive fracture energy(DIANAFEA). The compression stress-strain parameters were based on experimental data of Russell and Graybeal, and are summarized in Table 2.

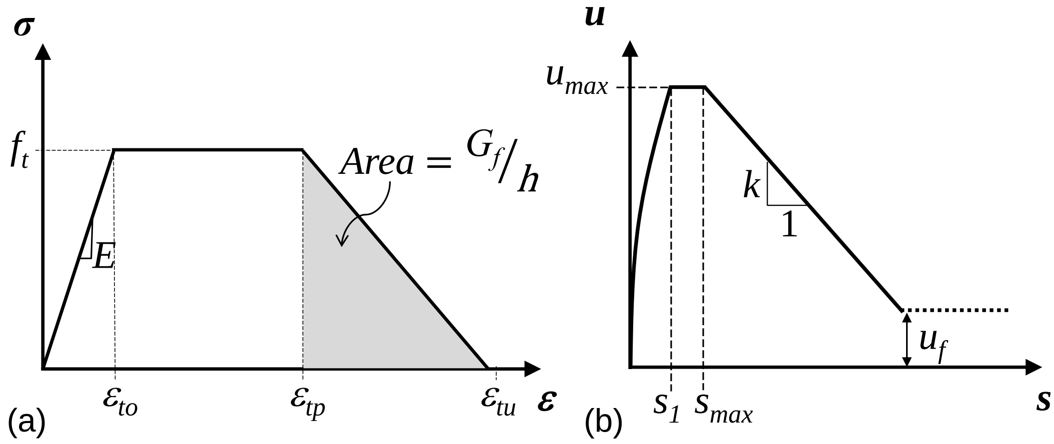

Figure 2. (a) Multilinear tensile stress-strain parameters (b) Bond-slip parameters

Table 2. Material Properties

Description	f_t [MPa]	ε_{to} [%]	ε_{tp} [%]	G_f [MPa-mm]	f_c' [MPa]	G_c [MPa-mm]	E [GPa]	ν	f_y [MPa]	f_u [MPa]	ε_u [%]
UHPC	8.0	0.0191	0.20	19	120	180	42	0.18	-	-	-
Longitudinal	-	-	-	-	-	-	200	0.3	455	690	16
Transverse	-	-	-	-	-	-	205	0.3	675	-	-

Longitudinal and transverse reinforcement were modeled as a truss element with an element size of 10 mm. The constitutive behavior of longitudinal reinforcement was modeled using the Von Mises plasticity strain hardening model for monotonic loading and simply supported beam models under cyclic loading. The longitudinal reinforcement in cantilever models under cyclic loading were modeled using a modified two-surface plasticity model which includes the Bauschinger effect essential to capture the hysteretic response in cantilever beams under cyclic loading. The tensile stress-strain curve parameters of the longitudinal and transverse reinforcement were based on the uniaxial tensile test conducted by Bandelt and Billington (Table 2). The interaction between longitudinal reinforcement and UHPC matrix was modeled through Bond-slip constitutive relationship proposed by Bandelt and Billington (Figure 2(b)). The bond-slip parameters such as maximum bond strength ($u_{max} = 10.4\, MPa$), slip at onset of softening ($s_{max} = 1\, mm$), bond-slip softening stiffness ($k = 1\, MPa/mm$), and residual friction bond strength ($u_f = 3.8\, MPa$) were obtained from bond-slip test data of Dagenais and Massicotte. The cyclic bond-slip parameters were adjusted to account for deterioration due to load cycling.

A nonlinear static analysis with an incremental displacement-based loading was used for the simulation. The details about the loading protocol has already been discussed in Section 2.1. The ultimate failure of the finite element models was due to the fracture of tensile longitudinal reinforcement in all the simulations. Fracture was assumed to occur when the strain over a 30 mm gage length of the longitudinal reinforcement exceeded an 18% threshold strain based on the approach outlined in the study by Bandelt and Billington. A regular Newton-Raphson scheme was used for equilibrium criteria and a line search algorithm was used for numerical convergence.

Convergence was assumed to have occurred at each iteration if either energy, displacement, or force norm did not exceed limiting values of 0.01%, 0.1% and 1%, respectively.

3. Analytical Method

3.1. Equivalent Plastic Hinge Length

To explain the theoretical formulation, a cantilever beam with shear-span, L_s, is subjected to a lateral load, P_u, such that it has ultimate displacement, Δ_u, as shown in Figure 3(a). The ultimate limit state curvature distribution of the cantilever would be highly non-linear (Figure 3(b)) with significant portion of longitudinal reinforcement near the critical section (i.e., section at which maximum moment occurs) exceeding the yield stress. This curvature distribution at ultimate level can be divided into two regions: elastic curvature and plastic curvature (shaded region).

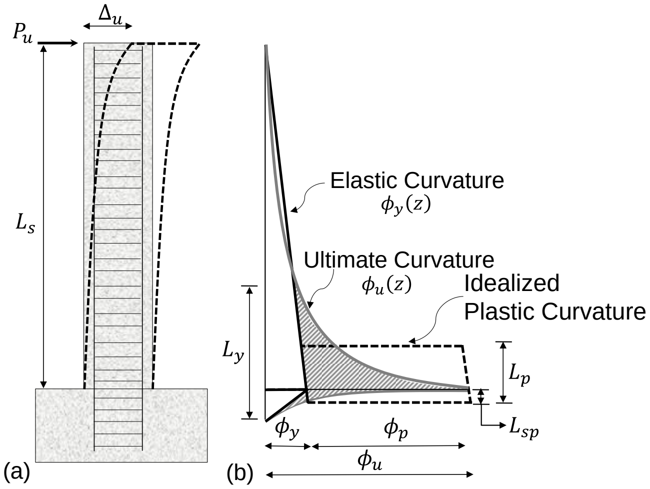

Figure 3. Theoretical formulation of equivalent plastic hinge length (a) cantilever beam with lateral load (b) curvature distribution

The plastic rotation can be calculated by integrating the plastic curvature along reinforcement yielding zone using Equation 3 (shaded region in Figure 3(b)).

$$\theta_p = \int_0^{L_y} [\phi_u(z) - \phi_y(z)] dz \tag{3}$$

Where $\phi_u(z)$ and $\phi_y(z)$ are the sectional curvatures of the beam at ultimate level and service level. Using the equal area principle, equivalent plastic hinge length can now be calculated by dividing the plastic rotation (obtained from Equation 3) by a constant or idealized plastic curvature (i.e., $\phi_p = \phi_u - \phi_y$) as shown in Equation 4.

$$L_p = \frac{\theta_p}{(\phi_u - \phi_y)} \tag{4}$$

Where ϕ_u and ϕ_y are the curvatures at critical section of the beams at ultimate level and service level, which were calculated using sectional analysis based on the plane section hypothesis, uniaxial stress-strain relationship, equilibrium of forces and strain compatibility.

3.2. Chord Rotation at Ultimate Level

The chord rotation at ultimate level (i.e., rebar fracture) was calculated using sectional analysis by extending the commonly used Euler-Bernoulli beam theory (i.e., plane section hypothesis, strain compatibility, equilibrium of sectional forces and uniaxial material model). The cross-section was assumed to have reached its ultimate limit state when the strain in tensile reinforcement reached the ultimate strain of 18%. This failure criteria at the ultimate limit state is based on recent experimental and numerical simulation study of reinforced HPFRCC under monotonic and reversed cyclic loading (Bandelt and Billington). In the sectional analysis, the contribution of UHPC in tensile component of sectional forces was considered to be zero due to crack localization at the critical section. Ultimate rotation capacity of the reinforced UHPC flexural member was computed as the sum of elastic or yield rotation (θ_y) and plastic rotation (θ_p) as defined in Equation 1.

4. Results and Discussion

4.1. Numerically Simulated L_p in reinforced UHPC

The equivalent plastic hinge length values (L_p) obtained from the numerical simulation technique were normalized by the effective depth (d) to compare with the plastic hinge length obtained through existing empirical equations as shown in Figure 4. The bar chart shows normalized plastic hinge length across various reinforcement ratio (ρ), shear span-to-depth ratio (L_s/d), and boundary condition. It can be observed that the numerically simulated plastic hinge length increased with the increase in reinforcement ratio under both monotonic and cyclic loading. The plastic hinge length obtained from simulation was found to be higher in cantilever setup compared to simply supported setup which is due to the penetration of tensile strain into the foundation through bond-slip phenomenon. The plastic hinge was found to marginally increase with the increase in shear span-to-depth ratio. Further, plastic hinge was found to be lower under cyclic loading compared to monotonic loading in majority of the simulated beams. This is due to the effect of reversed load cycling which causes exponential increase in plastic curvature within a short region of the simulated beam.

Comparison of the equivalent plastic hinge with the existing empirical equations shows that the numerically simulated plastic hinge ($L_p \approx 0.25d \ to \ 0.5d$) are lower than all the existing expressions ($L_p \approx 0.5d \ to \ 1.5d$) under both types of loading scenario. This difference can be attributed to the following: (1) two of the empirical equations were developed using reinforced concrete experimental data (Mattock; Paulay and Priestley) which do not capture the effect of crack localization and strain concentration under flexural loading as observed in reinforced UHPC specimens (Yoo and Yoon; Hung and Chueh); (2) L_p equation for reinforced HPFRCC members developed by Naaman et al. was based on reinforcement yielding zone which is always larger than the equivalent plastic hinge length; (3) L_p expression proposed by Tariq, Jampole, and Bandelt was based on the experimental data of engineered cementitious composite (ECC) which has a much lower tensile strength than UHPC and it was proposed based on a limited database of six specimens with few control variables. Therefore, the use of these existing expressions to estimate equivalent plastic hinge length can result in over-prediction of the plastic rotation capacity and ultimate rotation capacity in reinforced UHPC structural members as further discussed in Section 4.2.

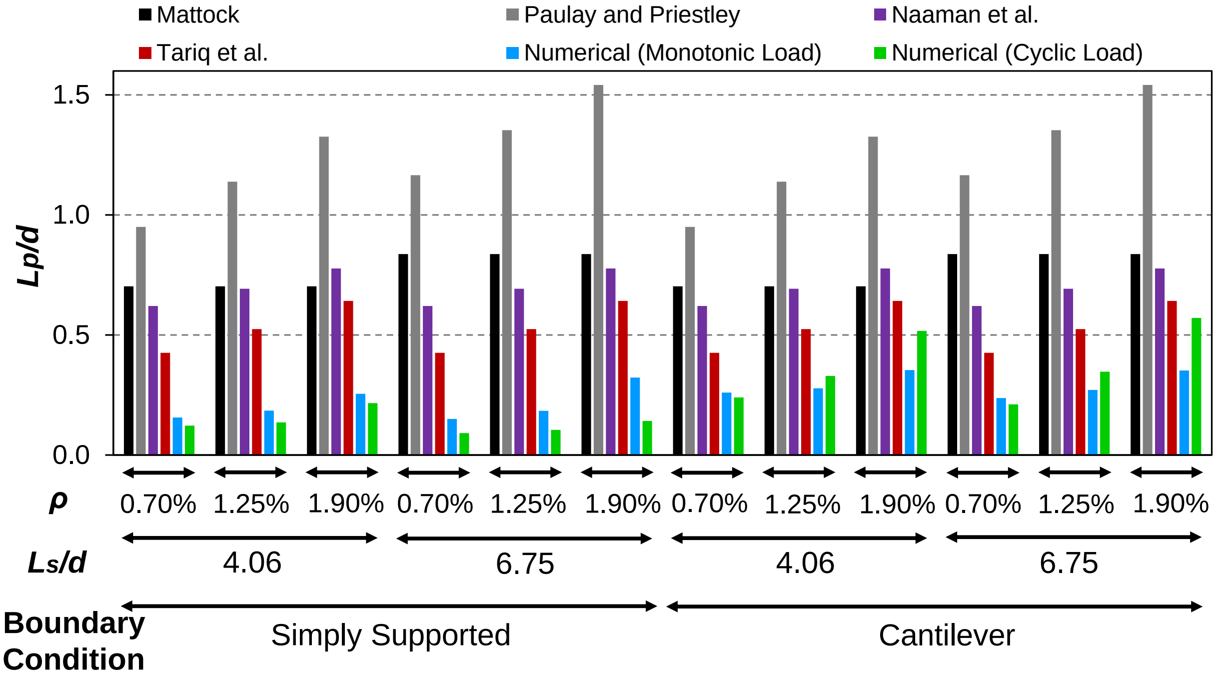

Figure 4. Comparison of equivalent plastic hinge length computed from simulation under monotonic and cyclic loading with that computed from existing empirical models

4.2. Ultimate Chord rotation

The ultimate chord rotation was calculated using the plastic hinge length values and sectional analysis as described in Section 3.2. To validate the ultimate chord rotation values obtained through the simplified mechanics, chord rotation was also computed by integrating curvature distribution along the shear-span of the beam using the strain data obtained from the numerical simulation. Figure 5 shows the comparison of the ultimate chord rotation computed using the analytical method (i.e., sectional analysis) and the numerical simulation. While using the existing plastic hinge length equations, it can be observed that the mean ratio (μ_{RATIO}) of analytical-to-numerically simulated value of ultimate rotation (θ_u) varies from 1.98 to 5.27 under two types of loading scenario. This indicates that the use of existing empirical equations significant over-predicts the component level ultimate rotation in reinforced UHPC members. The prediction scatter is also higher as shown by the coefficient of variation values ($19\% < CoV < 46\%$). However, with the use of plastic hinge length values obtained through the numerical technique, the ultimate chord rotation is well predicted ($\mu_{RATIO} = 0.99$) with low prediction scatter ($CoV = 3\%$) under both types of loading scenario.

5. Conclusions

A numerical simulation based technique was explored to calculate the equivalent plastic hinge length in reinforced UHPC flexural members under monotonic and cyclic loading. The existing empirical equations were found to significantly over-predict the plastic hinge length in simulated reinforced UHPC members. The use of numerically calculated plastic hinge length values combined with the sectional analysis was found to accurately predict the ultimate chord rotation in reinforced UHPC flexural members, whereas the use of existing plastic hinge length equations did not show good prediction capability.

Therefore, a new empirical equation is required to accurately compute equivalent plastic hinge length in reinforced UHPC flexural members by considering variation in all the potential predictor variables. The results of this study can be enhanced by incorporating additional variation in tensile and compressive properties in UHPC and performing a rigorous statistical analysis to propose a new expression for equivalent plastic hinge length.

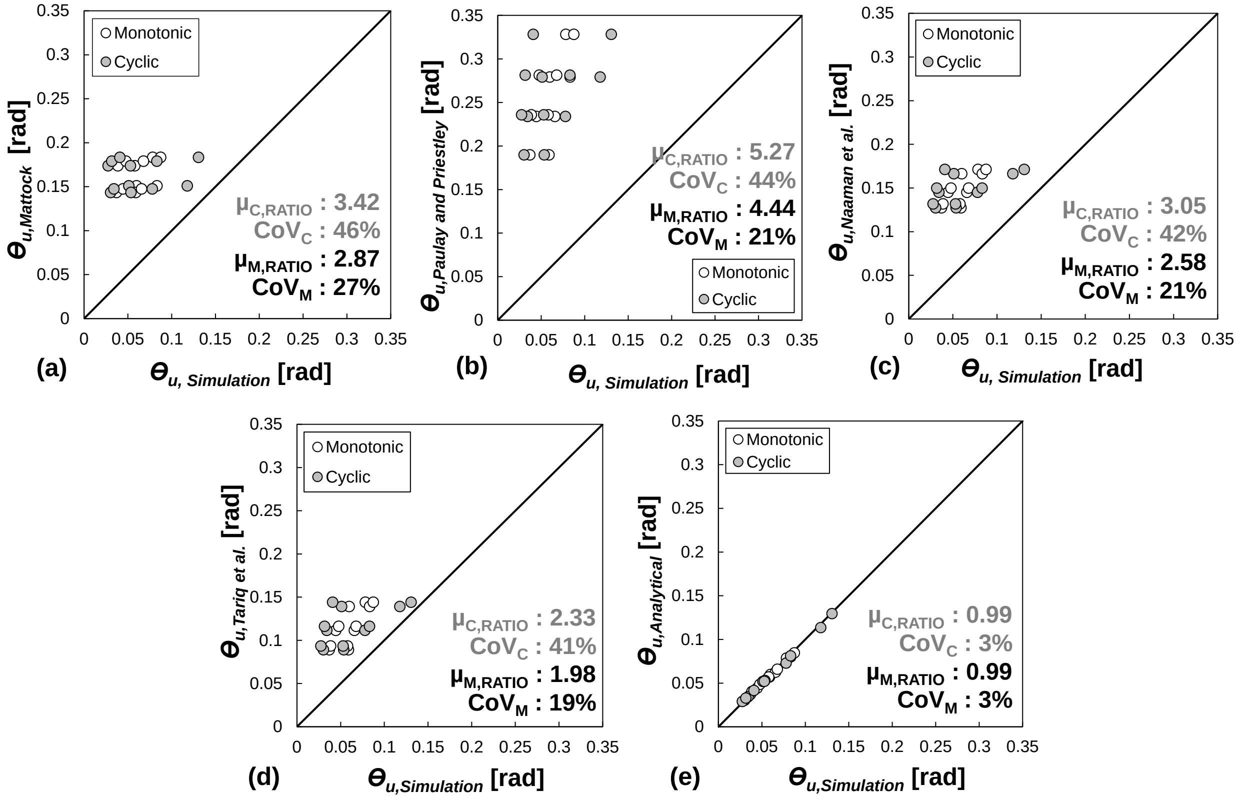

Figure 5. Comparison of ultimate rotation computed from simulation vs. analytical formulation using L_p from (a) Mattock (b) Paulay and Priestley (c) Naaman et al. (d) Tariq et al. (e) numerically calculated

6. References

Bandelt, Matthew J., and Sarah L. Billington. "Impact of Reinforcement Ratio and Loading Type on the Deformation Capacity of High-Performance Fiber-Reinforced Cementitious Composites Reinforced with Mild Steel." *Journal of Structural Engineering*, vol. 142, 2016, p. 04016084, doi:10.1061/(ASCE)ST.1943-541X.0001562.

Bandelt, Matthew J., and Sarah L. Billington. "Simulation of Deformation Capacity in Reinforced High-Performance Fiber-Reinforced Cementitious Composite Flexural Members." *Journal of Structural Engineering*, vol. 144, no. 10, 2018, p. 04018188, doi:10.1061/(ASCE)ST.1943-541X.0002174.

Dagenais, Marc-André, and Bruno Massicotte. "Cyclic Behavior of Lap Splices Strengthened with Ultrahigh Performance Fiber-Reinforced Concrete." *Journal of Structural Engineering*, vol. 143, no. 2, 2017, p. 04016163, doi:10.1061/(ASCE)ST.1943-541X.0001652.

DIANAFEA. *DIANA Release 10.2*. http://www.dianafea.com, 2017.

Feenstra, P. H., et al. “A 3D Constitutive Model for Concrete Based on a Co-Rotational Concept.” *Computational Modelling of Concrete Structures, Proceedings of EURO-C 1998,* edited by De Borst et al., Balkema, 1998, pp. 13–22.

Graybeal, Benjamin A. *Material Property Characterization of Ultra-High Performance Concrete*. PUBLICATION NO. FHWA-HRT-06-103, 2006.

Hung, Chung-Chan, and Chen-Yu Chueh. “Cyclic Behavior of UHPFRC Flexural Members Reinforced with High-Strength Steel Rebar.” *Engineering Structures*, vol. 122, Elsevier Ltd, 2016, pp. 108–20, doi:10.1016/j.engstruct.2016.05.008.

Mattock, Alan H. “Discussion of Rotation Capacity of Reinforced Concrete Beams.” *Journal of the Structural Division*, vol. 93, no. 2, 1967, pp. 519–22.

Naaman, A. E., et al. “Reinforced and Prestressed Concrete Using HPFRCC Matrices.” *High Performance Fiber Reinforced Cement 825 Composites 2 (HPFRCC 2),* edited by A.E. Naaman and H.W. Reinhardt, no. June, E & FN Spon, 1996, pp. 291–347.

Paulay, T., and M. J. Nigel Priestley. *Seismic Design of Reinforced Concrete and Masonry Buildings*. John Wiley & Sons,Inc., 1992.

Pokhrel, Mandeep, and Matthew J. Bandelt. “Material Properties and Structural Characteristics Influencing Reinforced HPFRCC Deformation Capacity and Plasticity.” *Submitted to Composite Structures*, 2018.

Priestley, M. J. N., et al. “Direct Displacement-Based Seismic Design of Structures.” *NZSEE Conference*, IUSS Press, 2007, pp. 1–23.

Reinhardt, A. E. Naaman H. W. *Proposed Classification of HPFRC Composites Based on Their Tensile Response*. 2006, pp. 547–55, doi:10.1617/s11527-006-9103-2.

Russell, Henry G., and Benjamin A. Graybeal. *Ultra-High Performance Concrete : A State-of-the-Art Report for the Bridge Community*. Vol. FHWA-HRT-1, 2013.

Tariq, Hasan, et al. “Fiber-Hinge Modeling of Engineered Cementitious Composite Flexural Members under Large Deformations.” *Engineering Structures,* vol. 182, Elsevier, 2019, pp. 62–78, doi:10.1016/j.engstruct.2018.11.076.

Wille, K., and Antoine E. Naaman. “Fracture Energy of UHP-FRC under Direct Tensile Loading.” *Fracture Mechanics of Concrete and Concrete Structures, Proceedings of FraMCoS-7*, edited by B. H. Oh and et al., 2010, pp. 65–72.

Yoo, Doo Yeol, and Young Soo Yoon. “A Review on Structural Behavior, Design, and Application of Ultra-High-Performance Fiber-Reinforced Concrete.” *International Journal of Concrete Structures and Materials*, vol. 10, no. 2, Korea Concrete Institute, 2016, pp. 125–42, doi:10.1007/s40069-016-0143-x.

---. “Structural Performance of Ultra-High-Performance Concrete Beams with Different Steel Fibers.” *Engineering Structures,* vol. 102, Elsevier Ltd, 2015, pp. 409–23, doi:10.1016/j.engstruct.2015.08.029.